Journal of Food Engineering 187 (2016) 1–13

Contents lists available at ScienceDirect

Journal of Food Engineering

journal homepage: www.elsevier.com/locate/jfoodeng

Non-destructive characterisation and quantification of the effect of conventional oven and forced convection continuous tumble (FCCT) roasting on the three-dimensional microstructure of whole wheat kernels using X-ray micro-computed tomography (μCT)

Letitia Schoeman [a], Anton du Plessis [b], Marena Manley [a, *]

[a] Department of Food Science, Stellenbosch University, Private Bag X1, Matieland, Stellenbosch, 7602, South Africa
[b] CT Scanner, Central Analytical Facility, Stellenbosch University, Private Bag X1, Matieland, Stellenbosch, 7602, South Africa

ARTICLE INFO

Article history:
Received 12 October 2015
Received in revised form
18 April 2016
Accepted 19 April 2016
Available online 22 April 2016

Keywords:
Microstructure
X-ray micro-computed tomography
Image analysis
Roasting
Porosity

ABSTRACT

Food microstructure influences the characteristics of end products. X-ray micro-computed tomography (μCT) enables investigating internal structure of food products non-destructively. High-resolution X-ray μCT, in combination with image analysis, was used to visualise and quantify the impact of conventional oven and forced convection continuous tumble (FCCT) roasting (180 °C for 140 s) on the microstructure of whole wheat kernels. After image acquisition, two-dimensional (2D) cross-sectional images were reconstructed into three-dimensional (3D) volumes. Quantitative parameters, i.e. volume, porosity, expansion ratio (ER) and relative density, were calculated. Oven roasting was associated with a significantly ($P < 0.05$) larger increase in kernel volume (4.47%) than FCCT roasting (1.57%). Porosity was higher in the oven-roasted samples (10.33 ± 4.63%), indicating a more destructive impact on the internal structure (FCCT = 8.29 ± 2.29%). Roasting introduced cavities and cracks within the wheat kernels, resulting in a decrease in whole kernel density (oven = 2.76%; FCCT = 0.55%), however the material density remained unaffected during FCCT roasting.

1. Introduction

Worldwide, wheat (*Triticum aestivum* L.) is an important crop, with total annual yields exceeding 700 million tonnes in 2013 (FAOSTAT, 2015). The success of wheat as a raw material can be attributed to its processing properties and its ability to develop cohesive doughs that can be formed into noodles and pasta or baked into bread (Lamacchia et al., 2010). Wheat is a staple food and is used for human consumption in a variety of products, i.e. breads, pastas, noodles, couscous, cakes, biscuits, pastries, breakfast cereals and flour.

Cereal roasting is traditionally practiced in India with the objective of increasing shelf life, enhancing organoleptic properties and to ease integration into breakfast cereals and other ready-to-eat products (Murthy et al., 2008). Most roasters used in India are batch type heated pans, where sand is used as heat transfer medium. This roasting method has various negative aspects since it is unhygienic, tedious to operate, leads to a low productivity, there is a lack of temperature control and the product has non-uniform characteristics (Murthy et al., 2008).

Few investigations focused on the effect of heat treatment on the microstructure of cereal grains; the effect of roasting specifically has been even less investigated. Gun puffing (105–115 °C) strongly influenced the kernel morphology and it led to an increased water holding capacity of the flour (Mariotti et al., 2006). Roasted wheat can be roller milled to obtain flour yields as high as 70–75% when the moisture content is below 10% (Lazar et al., 1974). Flour from roasted wheat can be included in breads, pastas, baked and fried speciality products, gels, batters, instant sauces, snacks, gruels and it can be used as basis for beverage products (Baiano et al., 2008; Lazar et al., 1974; Mossman et al., 1973).

A few studies reported on the use of a forced convection continuous tumble (FCCT) roaster for agricultural products such as marama beans and cowpeas (Kayitesi et al., 2010; Ndungu et al., 2012; Nyembwe et al., 2015). The FCCT roaster is an energy efficient roasting technique that can be used to modify the

* Corresponding author.
E-mail address: mman@sun.ac.za (M. Manley).

http://dx.doi.org/10.1016/j.jfoodeng.2016.04.015
0260-8774/

microstructure of cereal grains. This roaster employs the moisture inside the sample to generate superheated steam, leading to faster and even heat transfer. The rotating cylinder enables the sample to be suspended in the heated air, thus all the surfaces are exposed evenly to the heat. Thermal insulation results in less heat loss and efficient energy usage (Flinn, 2012).

In food science, it is common to relate physical behaviour to microstructure in order to gain more comprehensive insights into the product or production process. Food microstructure plays an important role in determining the characteristics (physical, textural and sensory) of the final product (Aguilera, 2005). Structural probing of also cereal grains are of great importance to the food industry, since microstructure effects processing, storage, functionality and the end use of products (Dogan, 2007). For example, the microstructure of wheat for bread making significantly influences its quality and baking properties. Traditionally, microstructural investigations involved light microscopy (LM), scanning electron microscopy (SEM) and confocal laser scanning microscopy (CLSM). These destructive methods however have various drawbacks. It requires sectioning which are likely to disrupt the structure, cause imaging artefacts and is limited to two-dimensional (2D) images (Salvo et al., 2010).

The limitations of 2D, destructive methods have led to the increasing use of a powerful non-destructive and non-invasive high-resolution imaging technique, X-ray micro-computed tomography (μCT), which enables characterisation of three-dimensional (3D) volumes for better understanding of food microstructure (Salvo et al., 2010; Zhu et al., 2012). X-ray μCT makes use of the differences in X-ray attenuation that arises mainly from differences in density within a sample. High density materials will attenuate the beam and areas of high attenuation will appear brighter on the 2D slice images. X-rays are sent around and through the scanned sample, creating projection X-ray images. Consecutive images are accumulated to create 3D volumes that can be manipulated digitally to perform a number of quantitative and qualitative measurements (Ketcham and Carlson, 2001).

Traditional computed tomography (CT) and μCT has been applied in various agricultural commodities e.g. traditional medical CT has been used to evaluate undesirable fibrous tissue in carrots (Donis-González et al., 2015) and to assess internal decay in fresh chestnuts (Donis-González et al., 2014), while μCT has been applied for 3D pore space quantification of apple tissue (Mendoza et al., 2007). Synchrotron X-ray CT was used to characterise the 3D gas exchange pathways in pome fruit (Verboven et al., 2008). Lammertyn et al. (2003) performed a comparative study using two non-destructive imaging techniques, X-ray CT and magnetic resonance imaging (MRI), to investigate the spatial distribution of core breakdown in pears.

X-ray μCT (40 kV; 250 μA) was recently investigated for real-time 3D visualisation and quantification of the internal structure of single wheat kernels damaged by sprouting and insect infestation (Suresh & Neethirajan, 2015). Other X-ray μCT cereal grain investigations include the characterisation of rice strains by differences in pore shapes (Zhu et al., 2012) and the effect of heat treatment on rice kernel structure (Mohorič et al., 2009; Witek et al., 2010).

It is not possible to examine expanded starch based products by conventional 2D imaging or scanning methods without destroying the structure. Cutting them also leads to disruption of the pores and breakage due to their brittle texture. To avoid these constraints non-destructive X-ray μCT were applied in a few studies for the characterisation of porous cereal products (Van Dalen et al., 2007), extruded products (Agbisit et al., 2007; Horvat et al., 2014), wheat flour dough (Bellido et al., 2006), bread (Besbes et al., 2013; Demirkesen et al., 2014; Van Dyck et al., 2014; Wang et al., 2011), and to explain airflow resistance in wheat (Neethirajan et al., 2006). Furthermore, X-ray μCT has been used widely to analyse porosity in food products, e.g. banana chips (Léonard et al., 2008) and meringues (Licciardello et al., 2012). Kelkar et al. (2015) recently described a method to determine the density of foods using X-ray μCT.

Andrejko et al. (2011) made use of X-ray radiographic examination to illustrate structural changes in wheat after infrared treatment (exceeding 150 °C and 90 s). High temperature roasting of coffee beans led to an increased volume and porosity and a decreased density with increase in roasting time (Frisullo et al., 2012). The ability to accurately analyse pores makes X-ray μCT an effective technique to study the microstructure of roasted products.

Quality changes occurring during thermal processing include sensory (flavour, odour and taste), optical (colour and appearance), structural (density, volume and porosity), textural, nutritional (proteins and vitamins) and rehydration properties (Vadivambal and Jayas, 2007). Roasting is a time-temperature dependant process that leads to chemical reactions, moisture loss and major changes in volume, shape and density (Hernández et al., 2008).

Wheat endosperm texture influences the energy requirement for milling. Porosity and density are closely related properties (Dobraszczyk et al., 2002) affecting endosperm texture and thus milling yield (Chang, 1988). More dense endosperm ground to larger particles which flows more easily and are easy to handle, whereas more porous endosperm mill to flours that are very fine and results in the blocking of mill sieves (Dobraszczyk et al., 2002). Ideally heat processing or roasting of wheat should have minimum effect on endosperm texture in terms of microstructural changes (porosity, volume and density). Decrease in material density would thus be undesirable. A roasting method resulting in adverse structural changes, i.e. larger cracks, large increase in porosity and loss in material density would be considered destructive.

Wheat kernel microstructural changes occurring during roasting have not been thoroughly studied in the pursuit of understanding the roasting phenomenon. The gap in understanding the mechanism that governs the behaviour of roasted grain microstructure is attributed to the lack of techniques capable of visualising the microstructure non-destructively. The need for 3D characterisation and quantification of microstructure, is now addressed with X-ray μCT which provides datasets that can be analysed for various structural parameters (Chevallier et al., 2014).

This study hypothesises that X-ray μCT is a feasible technique to determine the impact of roasting on wheat kernels. As verification this study presents the application of X-ray μCT in combination with image analysis to non-destructively investigate the impact of conventional oven and FCCT roasting on the microstructure of whole wheat kernels. Qualitatively the internal microstructure and porosity distribution were analysed using X-ray μCT 2D slice images and 3D volume renderings. Quantitative measurements, obtained from 3D volumes, included volume, porosity, expansion ratio (ER) and relative density.

2. Material and methods

2.1. Wheat samples

Eighteen whole wheat kernels were randomly selected from a wheat sample, kindly provided by PANNAR Seeds (Greytown, South Africa). The same kernels were imaged with X-ray μCT before (control) and after roasting to have a direct comparison. Nine kernels were subjected to oven roasting and nine to FCCT roasting. The kernels were weighed before and after roasting to determine the percentage weight loss. The samples were kept in sealed jars at ambient temperature until used.

2.2. Roasting

Wheat samples were roasted at 180 °C for 140 s using two roasting methods: conventional convection oven roasting (831 Electric Multifunction Thermofan Solid Plate Oven, Defy Appliances, Durban, South Africa) and FCCT roasting (Roastech, Bloemfontein, South Africa). For the FCCT roaster roasting time is determined by means of speed settings. A speed setting of 80 Hz is equivalent to 140 s and was used for FCCT roasting. This speed setting refers to the rotation speed of the screw conveyer inside the roasting chamber.

For both roasting methods the individual kernels were numbered for direct comparison of the X-ray images before and after roasting. The raw FCCT-roasted wheat kernels were in addition coloured with a heat-stable green dye to easily find the sample in each roasted batch. Each kernel was roasted, mixed in a 200 g rice sample. The nine kernels were roasted individually for each roasting method, thus nine replicates per roasting treatment.

The FCCT roaster has a capacity of 100 kg/h and the roasting chamber a volume of 0.199 m^3. A temperature of 180 °C was chosen since it falls within the thermal processing temperature range commonly used for cereal grains (Andrejko et al., 2011). A 15 min start-up time was allowed for the FCCT roaster to obtain steady-state conditions prior to roasting. The conventional convection oven was pre-heated to 180 °C before placing the numbered kernel in the oven together with 200 g of rice. The samples were placed centrally in the oven on a stainless steel baking tray. After roasting the samples were immediately cooled to ambient temperature by spreading it out on a cold flat surface to stop exothermic reactions and prevent excessive roast and further moisture loss. The samples were stored in airtight containers at ambient temperature until X-ray μCT image acquisition.

The main difference between the two roasting methods is that during oven roasting the sample is stationary, whereas during FCCT roasting the sample is continuously moving inside the roasting chamber. During FCCT roasting superheated steam is generated, since the moisture removed from the sample becomes part of the roasting medium (hot air) (Moreira, 2001). In the oven only dry, hot air is used as the moist air is replaced by fresh air that is heated to the desired temperature (Moreira, 2001). Superheated steam has been reported to be cleaner, cause less oxidation and colour deterioration and lead to a higher evaporation rate, thus mitigating the loss of nutritional values in comparison to hot air (Moreira, 2001).

2.3. X-ray micro-computed tomography (μCT) image acquisition

The wheat kernels were imaged under identical conditions (Table 1). Real-time X-ray μCT scans of the raw and roasted wheat kernels were obtained using a General Electric Phoenix V|Tome|X L240 (General Electric Sensing & Inspection Technologies GmbH, Phoenix, Wunstorff, Germany) high-resolution X-ray computed tomography system with a tungsten target X-ray tube. Due to X-ray μCT being non-destructive, the 3D internal structure of the same kernel could be studied before and after roasting.

Two wheat kernels, e.g. two raw, or one FCCT and one oven-roasted, were scanned together. Thus, for each of the nine oven and nine FCCT-roasted kernels, two scans were performed, firstly raw and then after being roasted. This was done in order to make direct comparisons between the kernels in the raw and roasted state. Various system settings were tested to optimise the scan quality. Instrumental conditions that needed to be considered included beam energy and current, sample-to-detector-distance and exposure time. Parameters were optimised to obtain the shortest possible scanning time while ensuring adequate image contrast. X-ray radiation was thus generated from a source voltage (energy) of 60 kV and an electron current set at 240 μA, resulting in CT scans with a voxel size (resolution) of 12 μm.

The scanning procedures described required no sample preparation, besides mounting of the sample. Each wheat kernel was mounted horizontally (crease facing down) on a piece of oasis (floral foam) and on a polymeric disc (10 mm thickness and 25 mm diameter), obtained from Maizey Plastics (Cape Town, South Africa), and glued to the translation stage (see sample setup in Fig. 1). The low density of the oasis made it an appropriate mounting material because it could easily be distinguished from the subject of interest. The density (2.15 g/cm^3) of the polymeric disc was used as a reference standard for relative density determinations; therefore the plastic was scanned in the field-of-view (FOV).

Table 1
Summary of the scanning parameters used for image acquisition.

Units	Parameter
Voltage (kV)	60
Current (μA)	240
Magnification	16.67
Pixel size in the X- and Y axes (mm)	0.200
Field-of-view (FOV) (mm)	700
Number of pixels in the X- and Y axes	2024
Resolution/voxel size (μm)	12
Spot size (μm)	5
Scan time (s)	1500
Original image greyscale intensity resolution	16-bit
Grey levels	$2^{16} = 65{,}536$
Number of 2D images	1500
Image acquisition time (ms)	500
Rotation sector (°)	360

2.4. Image processing and analysis

The 2D image slices, covering the entire sample were attained using a fully automated data acquisition system and saved onto a processing workstation, operated by system-supplied Datos reconstruction software (Datos|x® 2.1, General Electric Sensing & Inspection Technologies GmbH, Phoenix, Wunstorff, Germany). Angular projections generated 2D X-ray images which were reconstructed to create 3D volumes of the external and internal geometries of the sample. Reconstruction involved filtered back-projection algorithms. The final product from reconstruction is a raw 3D volume file which was imported directly into the image visualisation and analysis software (Volume Graphics VGStudio Max 2.2, Volume Graphics, Heidelberg, Germany).

2.4.1. Segmentation and defining regions-of-interest (ROIs)

Wheat kernel images were segmented into different ROIs: whole kernel, kernel material (which constitutes the solid phase) and air voids (which forms part of the gaseous phase). ROIs were subjected to the Volume analyser function (VGStudio Max 2.2) to calculate microstructural parameters. A representative slice from the kernels was selected from the dataset to obtain an average grey value for the solid and air components in the kernel. Once a segmented volume has been defined, quantitative measurements were performed.

2.4.2. Quantitative measurements

Quantitative measurements included volumes-of-interest (VOIs), porosity, expansion ratio (ER) and relative density. In addition, kernel dimensions (length, width and depth) were measured, also using VGStudio Max 2.2 software.

i. Volumes-of-interest (VOIs)

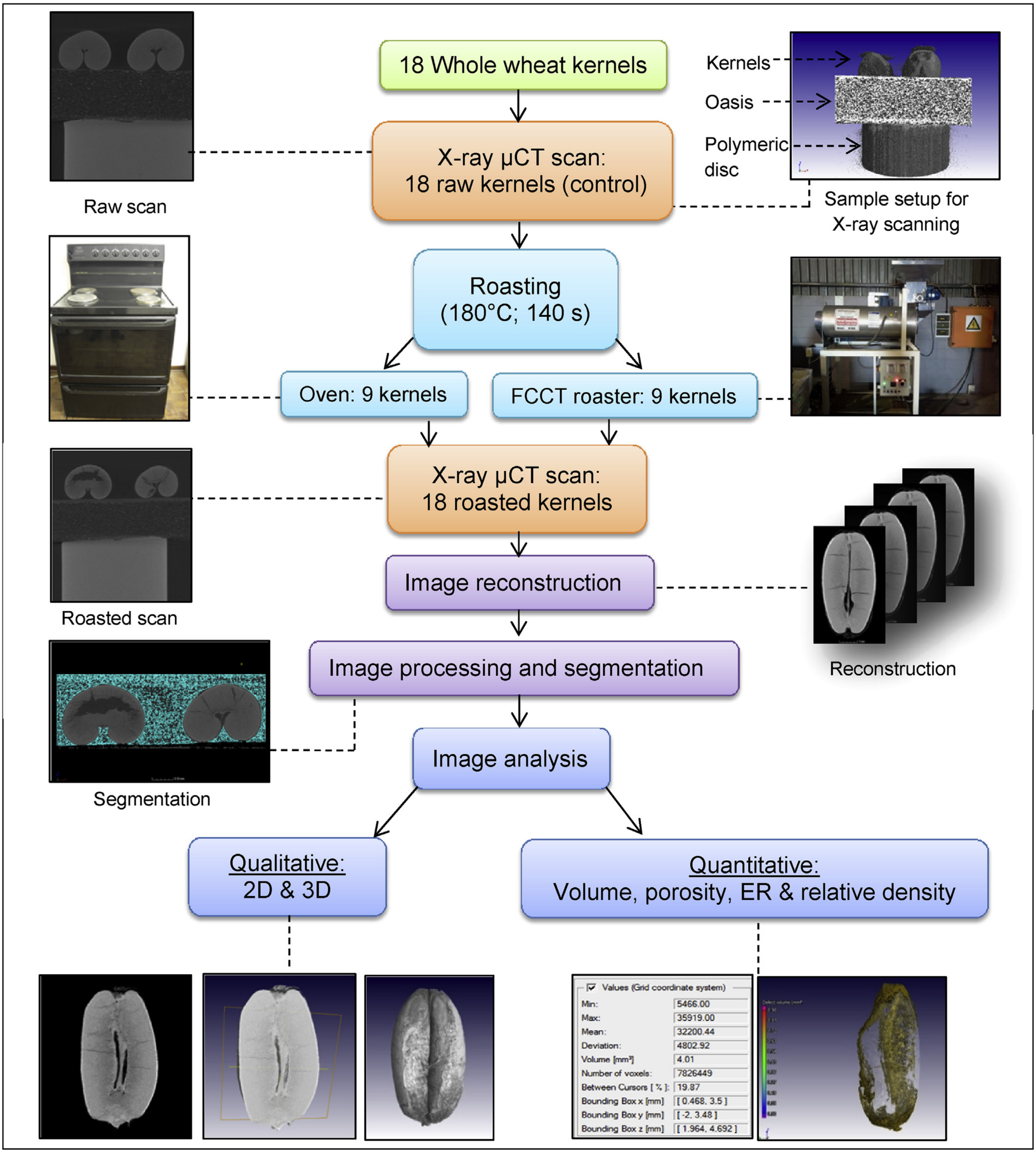

Fig. 1. Flow diagram of experimental design for determining the effect of oven and FCCT roasting on the microstructure of whole wheat kernels using X-ray µCT and image analysis.

VOIs were measured using the Volume analyser tool which automatically calculates the specific volume of the selected ROIs. By creating different VOIs, volume measurements of specific areas (e.g. air) in the sample or the sample as a whole can be determined.

ii. Porosity (percentage air volume)

Porosity is the ratio of the intergranular air space to the total space occupied by the kernel (Kheiralipour et al., 2008). Porosity analysis was performed by thresholding the voids and creating and extracting this ROI and calculating the total air volume against the total sample volume (Du Plessis et al., 2014). It should be noted that for this study the porosity were considered as the total air in the sample, thus the entirety of cavities and pores.

$$Porosity\ (\%) = \frac{Volume\ of\ air(mm^3)}{Total\ volume(mm^3)} \times 100\% \quad (1)$$

iii. Expansion ratio (ER)

$$ER = \frac{Volume\ after\ roasting\ (mm^3)}{Volume\ before\ roasting(mm^3)} \quad (2)$$

iv. Relative density

In this study relative densities were determined using mean grey values (arbitrary units) which correlate to the X-ray attenuation. Each voxel has a grey value which relies on the material density. Higher grey values, corresponds with higher attenuation coefficients and thus higher densities (Landis et al., 2003). The grey value histogram provides a diagram of the number and intensity of voxels in the whole image or specific ROI, illustrating the density distribution based on grey values (Landis and Keane, 2010). The y-axis display the number of voxels associated with each grey value, whereas the x-axis indicates the grey values and thus the intensity of the voxels in an image. Relative density was measured in terms of the mean grey value of the ROI in relation to the mean grey value of the reference standard. It was then multiplied with the known density of the reference standard (2.15 g/cm^3). For each ROI the mean grey value was measured using the Volume analyser tool. The mean grey value of the polymeric disc was attained by selecting a representative area using the Adaptive rectangle tool. The mean grey value of the homogenous polymer disc is thus a measure of its density.

$$Relative\ density\ \left(g/cm^3\right) = \frac{mean\ greyvalue\ of\ ROI}{mean\ greyvalue\ of\ reference\ standard} \times\ 2.15\ g/cm^3 \quad (3)$$

2.5. Experimental design

Fig. 1 details the experimental design for determining the effect of roasting on the microstructure of whole wheat kernels in a non-destructive manner by means of a flow diagram.

2.6. Statistical analysis

One-way analysis of variance (ANOVA) was performed to compare averages for the respective quantitative measurements with respect to the two roasting methods. Data was reported as the mean ($n = 9$) ± standard deviation. Data analyses were performed using STATISTICA version 13 (StatSoft, Inc., Tulsa, USA). The level of confidence required for significance was selected at $P < 0.05$.

3. Results and discussion

3.1. Visual assessment

The wheat kernels partially retained a brown/yellowish pigmentation due to the carotenoid content, despite the roasting method (Fig. 2). Roasting led to swollen grains with a widened crease, especially during oven roasting. Wheat with a more open crease require less force during milling than those with a closed crease (Evers and Millar, 2002). Furthermore, a more bulged appearance was observed in the oven-roasted samples, whereas the FCCT-roasted kernels remained more uniform in shape. The bran outer layer, which surrounds the germ and endosperm, remained intact.

The digital images in Fig. 2 depict the cross-sectional views of raw, FCCT and oven-roasted wheat kernels. Since similar results were obtained, images of only one of the kernels for each roasting method are shown. The raw kernel had no visible internal cracks, whereas the FCCT-roasted kernel revealed thin cracks. In the oven-roasted kernel a large irregular internal void developed in the dorsal (non-crease) region. The appearance of the oven-roasted sample was similar to the internal structure obtained after roasting with a direct gas-fired pilot plant toaster (Lazar et al., 1974). The development of large internal voids resulted in a reduced toasted quality. The large cavity scatters the light reflected from the endosperm (Dobraszczyk et al., 2002) causing the oven-roasted wheat kernel to have a mealy and opaque appearance. Opaqueness is usually correlated with softness in wheat kernels since the air spaces leads to a decreased density (Almeida-Dominguez et al., 1997). The raw kernel appeared more translucent and the oven-roasted kernel was more opaque, whist the FCCT-roasted sample maintained a degree of translucency. The endosperm of the raw sample appeared white, while those of the FCCT and oven-roasted samples were greyish brown and yellowish white, respectively. Oven roasting resulted in a much darker, yellow-brown, external colour, while the FCCT-roasted sample retained a light brownish colour. This indicated the more intense degree of roasting using the oven roasting method, under similar conditions.

3.2. Qualitative image analysis

Qualitative analysis enables visualisation of the internal structure of the raw, FCCT and oven-roasted wheat kernels. A representation of the grey level 2D cross-sectional images, virtually cut in the middle for the three orthogonal views, i.e. frontal, horizontal and sagittal, is presented for the kernels before and after roasting in Fig. 3. Images of only one of the kernels for each roasting method are shown, since similar qualitative results were obtained.

3.2.1. Porosity, internal cracks and cavities (2D analysis)

The qualitative results illustrated considerable structural changes during roasting, especially in the oven-roasted kernels (Fig. 3). The raw samples were compact (dense) with few thin cracks and small cavities detectable. FCCT-roasted kernels contained slightly more and wider cracks, whereas the oven-roasted kernels had large cavities in the endosperm tissue especially near the centre of the kernel. These adverse changes resulted in the endosperm becoming completely unstructured. The endosperm is especially a crack sensitive region (Dobraszczyk et al., 2002). Small voids in the raw kernels are planes of weakness, which leads to the concentration of stresses, in this case internal pressure, and acts as sites where cracks or cavities initiate (Dobraszczyk et al., 2002). In the crease region, the wheat endosperm adheres peripherally to adjacent tissue, where a void (known as the endosperm cavity) exists (Evers and Millar, 2002). This endosperm cavity in the raw kernel can clearly be observed in the frontal views.

For both roasting methods, the bran remained intact, in spite of internal cracks (FCCT-roasted) and cavities (oven-roasted) formed in the endosperm. From the images, the aleurone layer appeared to be the densest constituent being the brightest region.

The germ remained intact as the cracks did not propagate into this region. From the sagittal orientation (Fig. 3), fissures can be observed as vertical lines in the oven-roasted endosperm. From this

Fig. 2. Digital (Canon SX40 digital camera, Canon, Ohtaku, Tokyo, Japan) images of the same wheat kernels before and after roasting with (a) and (b) raw, (c) and (d) FCCT-roasted, (e) and (f) raw, and (g) and (h) oven-roasted. The cross-sectional digital images of (i) raw, (j) FCCT-roasted and (k) oven-roasted kernels reveals the internal structure.

view, expansion of the roasted kernels is clear with oven roasting revealing much greater expansion compared to FCCT roasting. FCCT roasting had a less invasive impact on the internal structure in comparison to oven roasting which led to larger fissures.

During roasting air is incorporated into the structure due to physical and chemical changes taking place (Köksel et al., 1998). Internal moisture is transformed into the vapour state and the dense structure of the wheat kernel leads to an increase in vapour pressure resulting in the generation of steam and consequently expansion in structure. In the oven-roasted kernels sufficient pressure was generated to create large cavities in the cellular matrix. An inherent problem associated with oven roasting is non-uniform heating due to the uneven distribution of heat, in comparison to FCCT roasting where more uniform roasting is achieved.

The different modes of heat transfer in the roasting methods could be considered as the main factor responsible for the structural differences between the samples, since the roasting conditions (time and temperature) were similar. Continuous movement of the kernels in the rotating cylinder of the roasting drum of the FCCT roaster resulted in more uniform heat transfer. In contrast, during oven roasting the kernels were stationary and only the dry air was moving. FCCT roasting can be controlled by means of the rotating speed of the cylinder; a higher speed results in a faster roasting time. The internal steam generated inside the roaster together with the rotating movement of the cylinder lead to a more homogenous roasting process, where the superheated steam generated forms part of the heat transfer medium and is more evenly dispersed around the sample.

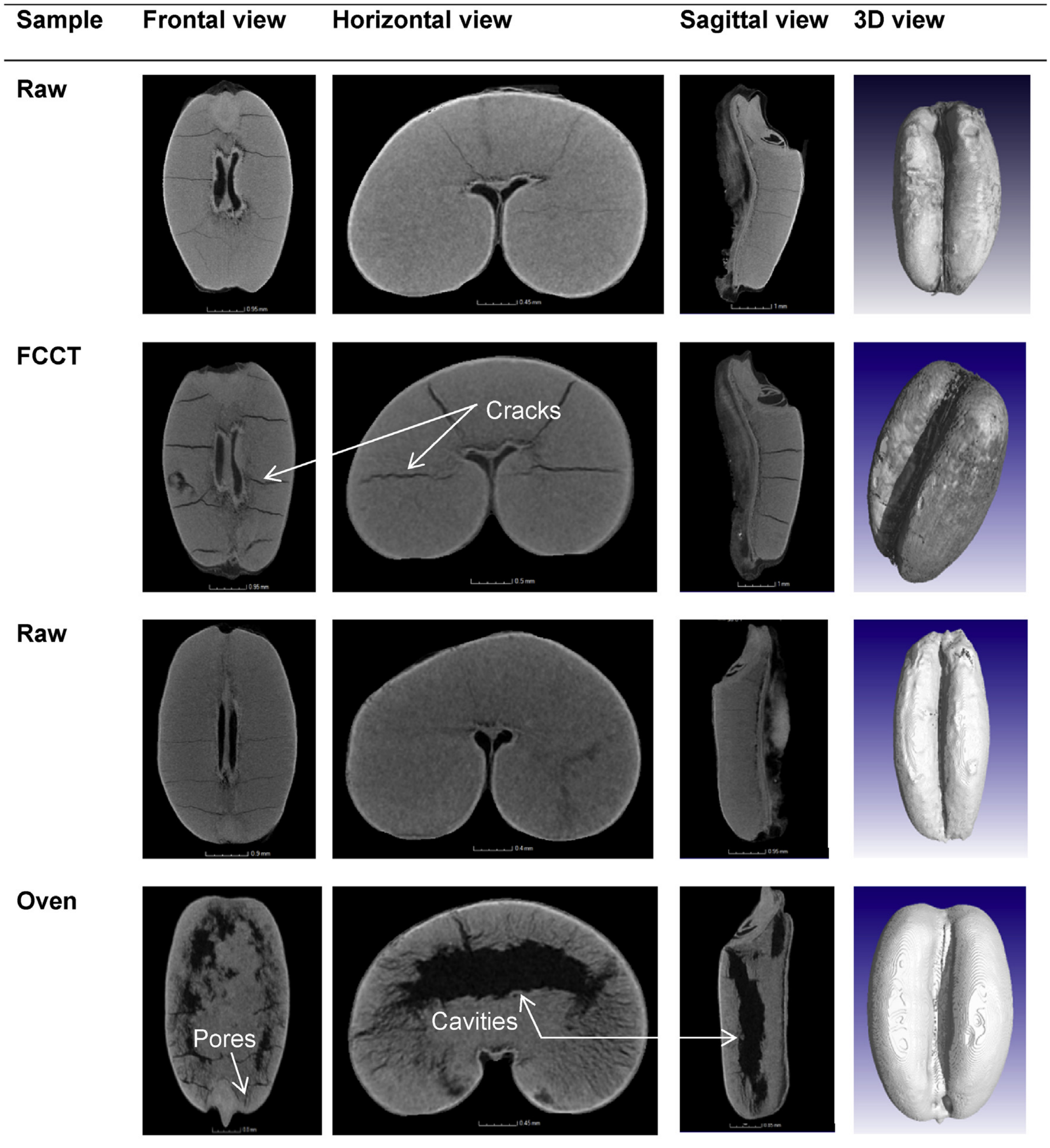

Fig. 3. Grey scale 2D tomographic images of the different views (frontal, horizontal and sagittal) of whole wheat kernels before and after FCCT and oven roasting (average dimensions: length = 6.02 ± 0.38 mm; width = 3.32 ± 0.27 mm; depth = 3.22 ± 0.32 mm).

Fig. 4 illustrates the three orthogonal views of the porosity in raw and roasted samples with the voids as ROI. Porosity describes the overall open structure of a desiccated material, where it comprises the fraction of empty volume. Raw wheat kernels displayed a dense internal structure with low porosity and more homogeneous distribution of the grey values (Fig. 4). The few small pores or cracks could be attributed to the drying process after harvesting. In the oven-roasted kernels fissures extended to close to the bran, however the outer layer remained intact, supporting the pores and large cavities. The large irregular distributed and partially interconnected cavities and cracks form a porous structure. The internal structure of the FCCT-roasted wheat kernels were characterised by multiple thin cracks.

Oven roasting had a more detrimental effect on porosity, being the more severe roasting method due to more direct heat penetration. This is in agreement with a wheat study where SEM images indicated that hot air roasted wheat has a greater porosity resulting in a reduced energy requirement for grinding (Murthy et al., 2008).

Cavities are like excavated cells, which are structured in a skeleton made by partial thermally degraded structures and the complete loss of the cell walls in some points. During roasting it can be assumed that smaller pores and cracks (FCCT-roasted) were formed due to the internal pressure created, and then ultimately the coalescence of these pores led to the development of larger asymmetric voids that resembles interconnected cavities (oven-roasted) (Pittia et al., 2011). These cavities are generated by a flash of superheated steam, which partially damages the structure (Sumithra and Bhattacharya, 2008). Cracks propogated from the centre outwards, with the largest areas of porosity towards the

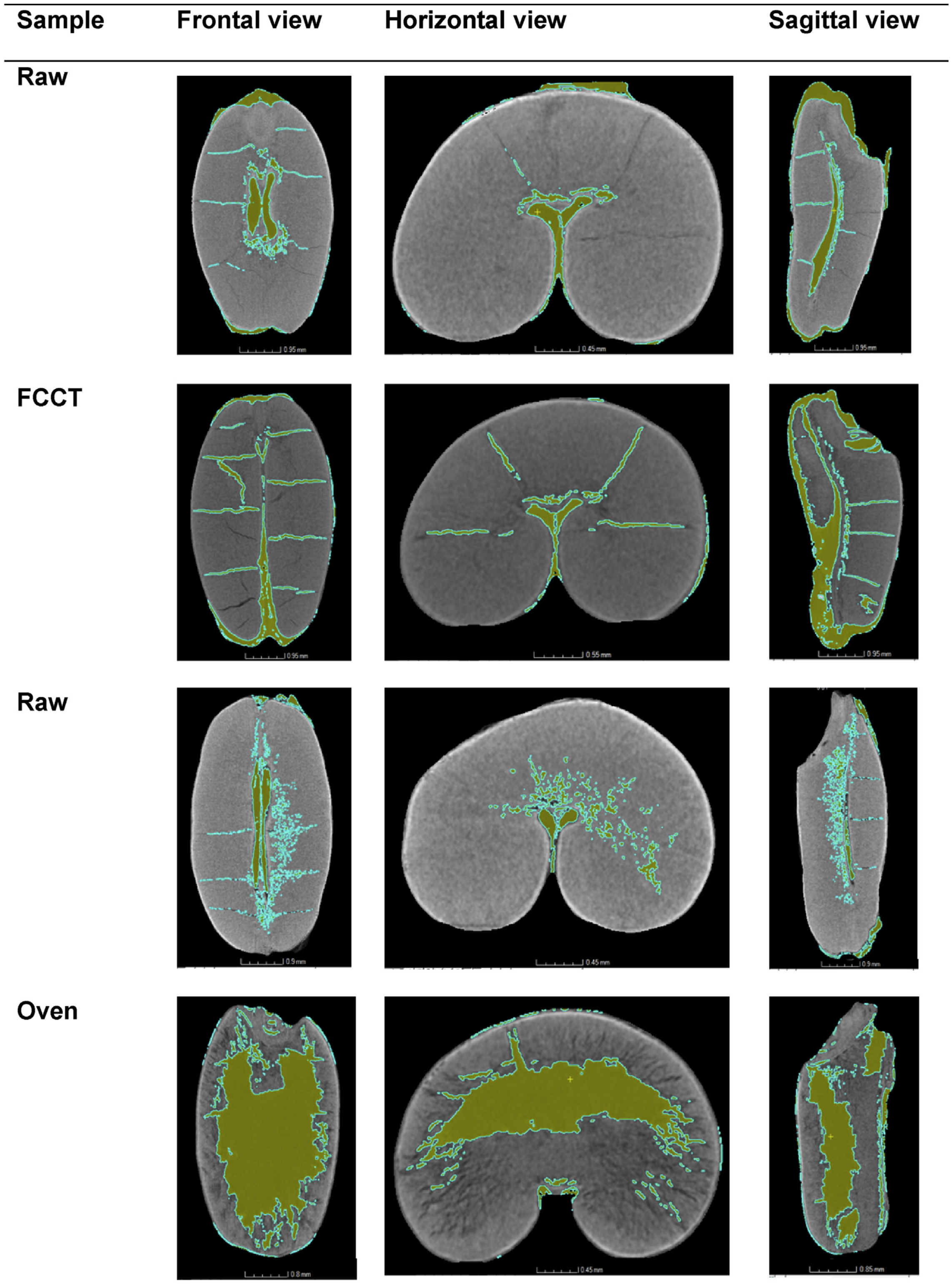

Fig. 4. 2D slice images (centre slice) of the spatial distribution of the porous network in wheat kernels before and after roasting, with the voids (total air) selected as ROI. The air filled pores and cavities are displayed in yellow and outlined with blue, while the kernel matrix is grey (average dimensions: length = 6.02 ± 0.38 mm; width = 3.32 ± 0.27 mm; depth = 3.22 ± 0.32 mm). (For interpretation of the references to colour in this figure legend, the reader is referred to the web version of this article.)

centre of the kernel, especially in the oven-roasted samples. This confirms that the thermal centre is localised in the centre of the wheat kernel (Andrejko et al., 2011).

3.2.2. Porosity, internal cracks and cavities (3D analysis)

Determining defects such as voids and cracks in a sample would typically require destructive testing. Volume rendering in 3D is required to understand the overall structure of samples and to visualise the internal microstructure (Suresh and Neethirajan, 2015). X-ray μCT scanning enables the detection of internal features and flaws by displaying this information in 3D without destroying the sample. In Fig. 5 the 2D images (a-c) and a 3D volume rendering (d), illustrates the internal porosity in a raw wheat kernel. The degree of porosity can be incorrectly interpreted from the 2D images as disconnected cavities. In the 3D volume rendering the path of the fissures or cracks are illustrated as tortuous and it contains multiple branching which creates an interconnected porous network throughout the kernel.

3.3. *Quantitative analysis*

Quantitative information on the internal structure can be obtained as volume, porosity and relative density whereas the geometry can be quantified in terms of size, shape, orientation and position. For quantitative density and volume measurements it is assumed that wheat kernels are a two-phase system with a solid phase (kernel structure) and a gas phase (voids).

3.3.1. *Volumes-of-interest (VOIs)*

Whole kernel and air volumes increased during roasting (Table 2). The increase in whole kernel volume (1.57%) was not significant ($P > 0.05$) during FCCT roasting in comparison to a significant ($P < 0.05$) increase of 4.47% during oven roasting. Both roasting methods resulted in a significant ($P < 0.05$) increase in air volume. The larger increase in whole kernel volume was due to the larger increase in air volume during oven roasting (103.38%). The increase in air volume was much lower for the FCCT-roasted samples (38.86%). The increase in whole kernel volume for both methods were lower than in a previous study where wheat roasted in a steel pan led to a 8.30% increase in kernel volume (Işikli et al., 2014). The increase in volume is due to the release of water, CO_2 and volatile organic compounds from the kernel to the gas phase (Dutra et al., 2001).

Thermal treatment of whole wheat kernels is typically associated with an increase in volume and a negative change in density (Bayram et al., 2004), with the large fissures contributing significantly to the increased volume of the expanded kernel (Pardeshi and Chattopadhyay, 2010). Fig. 6 displays the wheat kernel ROIs (whole kernel and air) to obtain the whole kernel and air volumes, respectively in a raw and oven-roasted sample.

3.3.2. *Porosity analysis*

Voids are inherent to wheat kernels and other cereal grains because of the porous nature of the endosperm (Chang, 1988). Thus, an increase in the existing porosity and development of additional voids were expected due to roasting. Understanding the contribution of air to the total wheat kernel is relevant because it affects the yield, which is a highly desirable property for the milling industry.

Porosity did not change significantly ($P > 0.05$) during FCCT roasting, however increased significantly ($P < 0.05$) during oven roasting. The porosity in the FCCT-roasted samples was 6.04 ± 1.54% and 8.29 ± 2.29% for the raw and roasted kernels respectively, resulting in a much lower increase (37.25%) than in the oven-roasted (95.64%) samples which ranged from 5.28 ± 1.57% to 10.33 ± 4.63%. FCCT roasting will result in a better quality roasted

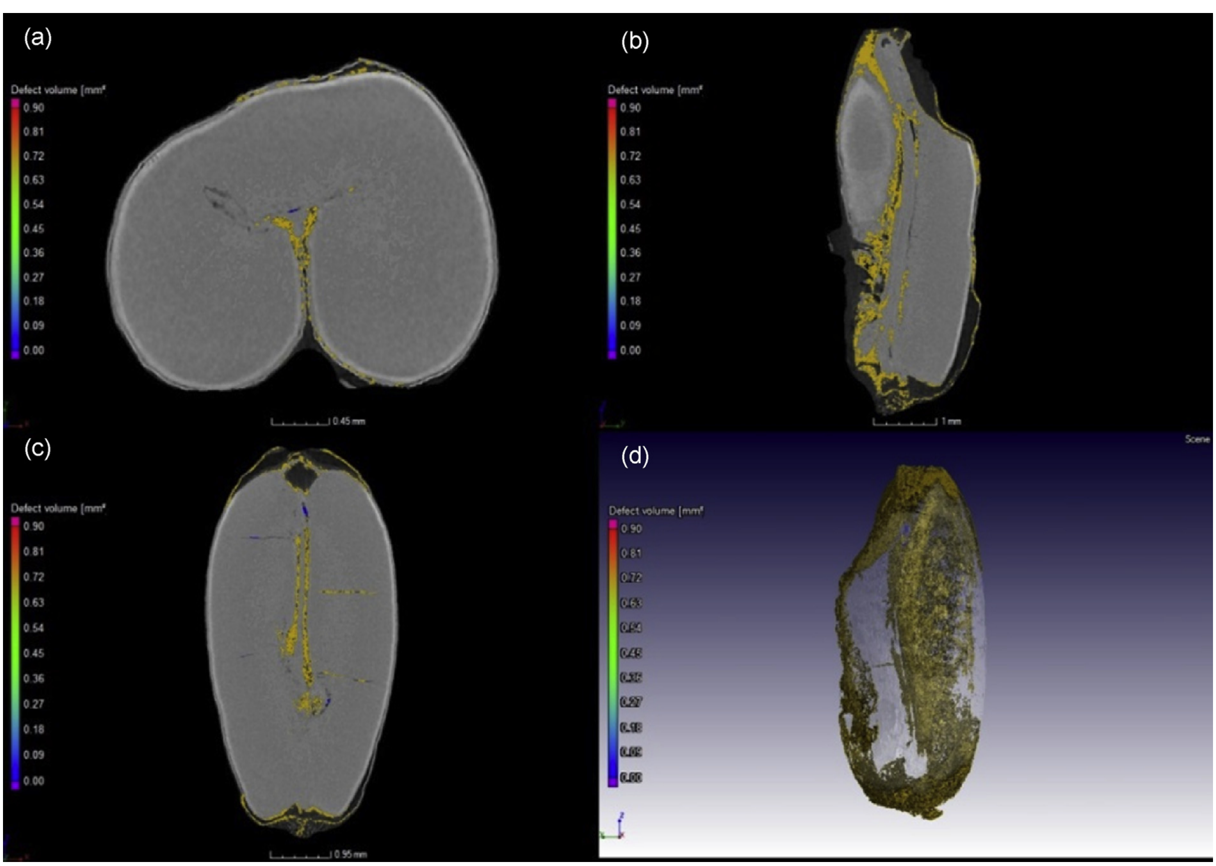

Fig. 5. 2D images (a-c) [(a) horizontal, (b) sagittal and (c) frontal views] and 3D volume rendering (d) of the porosity in a raw wheat kernel. In the 3D volume the visualisation of the porosity volume size distribution is characterised in yellow and the kernel structure (material) is represented as transparent (kernel dimensions: length = 5.46 mm; width = 2.59 mm; depth = 2.70 mm). (For interpretation of the references to colour in this figure legend, the reader is referred to the web version of this article.)

Table 2
Mean and percentage increase/decrease in microstructural parameters of wheat kernels before and after roasting.

Parameter	FCCT			Oven		
	Raw (n = 9)	Roasted (n = 9)	% Increase/Decrease	Raw (n = 9)	Roasted (n = 9)	% Increase/Decrease
Whole kernel VOI (mm^3)	29.24 ± 3.04^{ab}	29.70 ± 3.12^{ab}	1.57	28.40 ± 6.03^{b}	29.67 ± 5.66^{a}	4.47
Air VOI (mm^3)	1.75 ± 0.41^{b}	2.43 ± 0.58^{a}	38.86	1.48 ± 0.55^{b}	3.01 ± 1.27^{a}	103.38
Porosity (%)	6.04 ± 1.54^{cb}	8.29 ± 2.29^{ab}	37.25	5.28 ± 1.57^{c}	10.33 ± 4.63^{a}	95.64
Expansion ratio (ER)	1.02 ± 0.01^{a}		–	1.05 ± 0.06^{b}		–
Whole kernel relative density (g/cm^3)	1.81 ± 0.03^{a}	1.80 ± 0.03^{ab}	−0.55	1.81 ± 0.04^{a}	1.76 ± 0.07^{b}	−2.76
Material relative density (g/cm^3)	1.84 ± 0.03^{a}	1.84 ± 0.04^{a}	0	1.84 ± 0.04^{a}	1.79 ± 0.06^{b}	−2.72
Weight loss (%)	3.50 ± 3.68^{a}		–	6.04 ± 4.42^{a}		–

Values are means ± standard deviation, of nine replicates. Different letters in the same row indicate significant differences ($P < 0.05$).

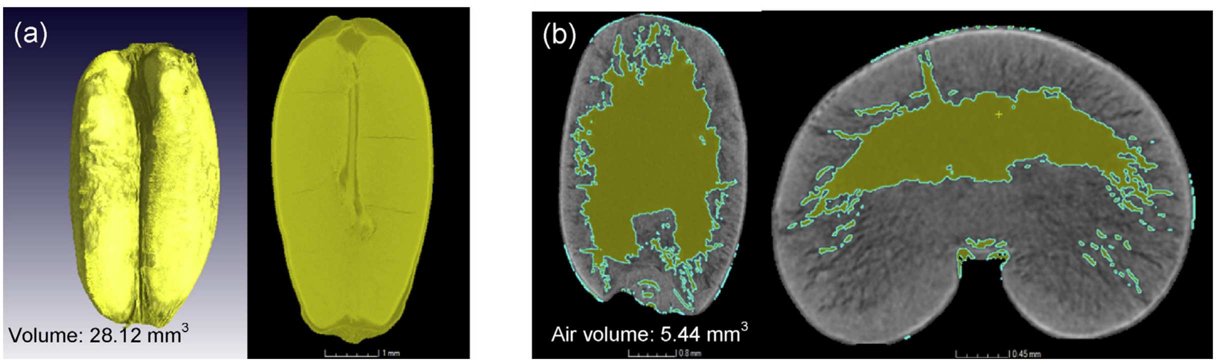

Fig. 6. Illustration of the use of the Volume analyser tool on a (a) raw sample where the whole kernel was selected as VOI (28.12 mm^3) and (b) oven-roasted sample where the air (yellow) was selected as VOI (5.44 mm^3) (kernel dimensions: length = 6.24 mm; width = 3.56 mm; depth = 3.27 mm). (For interpretation of the references to colour in this figure legend, the reader is referred to the web version of this article.)

product in terms of endosperm texture (too soft kernels are undesirable). The increased porosity during oven roasting can be ascribed to a bigger puffing effect occurring due to the higher internal vapour pressure generated. The greater porosity was consistent with the larger distributed internal network of cavities observed during qualitative analysis.

3.3.3. Expansion ratio (ER)

The ER is also known as the puffing index (PI) (Lazar et al., 1974). Larger ERs implies a larger difference in kernel volume before and after roasting. Greater air volumes correspond to greater ERs in cereal products (Jones et al., 2000; Sumithra and Bhattacharya, 2008). The oven-roasted kernels had the highest ER (1.05 ± 0.06) and porosity (10.33 ± 4.63%), compared to the FCCT-roasted samples (ER = 1.02 ± 0.01; porosity = 8.29 ± 2.29%) under similar roasting conditions (Table 2).

In infrared treated wheat (100–180 °C; 30–150 s) a negative relationship occurred between ER and density (Andrejko et al., 2011). This trend was also observed during oven roasting, where higher expansion was correlated to a higher relative density decrease (2.76%), while the FCCT-roasted kernels had a lower ER and a lower density decrease (0.55%).

A PI (using a gas-fired hot air toaster) of 1.3 was obtained for wheat kernels (15% moisture content) roasted at 204 °C for 17 s, whereas 40 s resulted in a PI of 1.5 (Lazar et al., 1974). The differences in ER values obtained can be attributed to the different roasting methods and conditions, and also to the moisture content. In the present study lower ERs were obtained due to the lower moisture content since no tempering was performed before roasting. Although roasting was conducted at a low moisture content, the combination of high temperature for a short duration will rapidly release steam resulting in an expanded structure (Sumithra and Bhattacharya, 2008). When the moisture content is too low, insufficient superheated vapour is generated, resulting in even lower ERs (Lee et al., 2000). This is, however, also dependent on the roasting method and conditions. The pericarp may also limit the degree of expansion (Mariotti et al., 2006).

3.3.4. Density analysis

Density determinations usually performed in industry include hectolitre mass, which provides limited information since only the average apparent density of the bulk is measured and it is influenced by the degree of packing and the shape and size of the crease (Dobraszczyk et al., 2002). Wheat density can also be measured using a pycnometer (Chang, 1988; Nelson, 2015; Ohm et al., 1998). Chang (1988) documented the mean true density of wheat to be 1.47 g/cm^3 and the mean apparent (inclusion of air) density as 1.39 g/cm^3. As some intercellular spaces are inaccessible to the gas or mercury, the volume determined using a pycnometer may include these air spaces and thus the density determined might not be the true density (Chang, 1988). Kelkar et al. (2015) developed a method, using both X-ray digital radiography and CT to directly determine the apparent density of foods. X-ray CT gave results comparable with conventional methods.

Fig. 7 demonstrates the grey value histograms for FCCT and oven-roasted wheat kernels. Two histograms are displayed for each roasting method (Fig 7): whole kernel and the air as ROI. A histogram with a wide distribution (Fig. 7a) indicates more contrast in the image, whereas a narrow distribution (Fig. 7c) correlates with less contrast (Umbaugh, 2011). If grey values are concentrated at the lower end of the graph (Fig. 7d), the image appears darker and vice versa. The whole kernel grey value histogram illustrate different peaks (corresponding to different phases), recognising that lower grey values correspond to internal air and higher values correspond to the kernel structure.

The mean grey values for the FCCT and oven-roasted samples

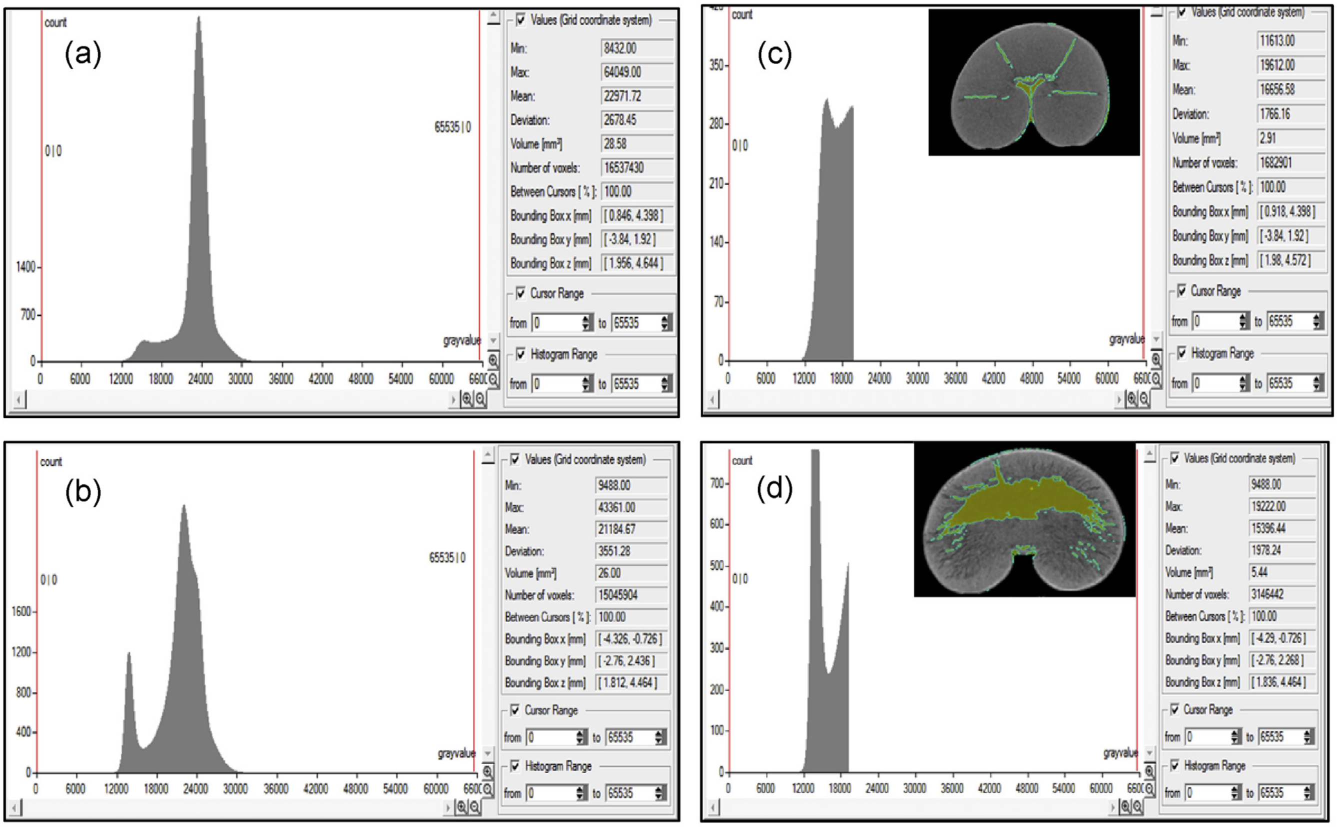

Fig. 7. Histograms illustrating the grey value distribution in images of whole (a) FCCT-roasted and (b) oven-roasted kernels and the air selected as ROI in (c) FCCT-roasted and (d) oven-roasted kernels. The top three values in the tables indicate the minimum, maximum and mean grey values, respectively.

were 22,971.72 and 21,184.67 respectively (Fig. 7a and b). The mean grey value intensity is a measure of brightness and density, where roasting resulted in lower mean grey values relating to lower densities of the roasted kernels. In the histograms the grey value range was smaller for the oven-roasted (9488-43361) sample than for the FCCT-roasted (8432-64049). The histogram of the oven-roasted kernel had more distinct peaks, indicating the increase in porosity due to the increase in the lower grey value peak (Fig. 7b). This large distribution of low grey values was also observed in the histogram where the air was selected as ROI (Fig. 7d) and is associated with more voids. Changes in the grey values associate with changes in the microstructure as observed during qualitative analysis.

Whole kernel density is the density of the kernel including air voids and thus it is a function of the air volume proportion (Vadivambal and Jayas, 2007), whereas the material density reports the density of the kernel material per se, excluding all the air, and is thus more representative of the true density. Whole kernel density decreased with 0.55% ($P > 0.05$) and 2.76% ($P < 0.05$) during FCCT and oven roasting, respectively (Table 2). In contrast, the material density remained unaffected during FCCT roasting while a significant ($P < 0.05$) decrease of 2.72% occurred during oven roasting. The significantly larger decrease in whole kernel density during oven roasting was due to the higher porosity that developed using this method. These results were in agreement with previous studies that suggested lower densities were due to higher porosities, expansion (volume increase) and as a result of moisture loss (Al-Mahasneh and Rababah, 2007; Fang and Campbell, 2000; Jha, 2005). Whole kernel densities were lower than material densities because it included the contribution of air which lowered the density. The weight loss for the oven-roasted samples was much higher with an average of 6.04 ± 4.42%, whereas FCCT roasting contributed to a loss of 3.50 ± 3.68% (Table 2).

Murthy et al. (2008) investigated the impact of fluidised bed roasting (FBR) (280–350 °C for 30–120 s), using hot flue gas as fluidising medium and traditional pan roasting (300 °C for 15–100 s), using sand as heat transfer method on the quality of wheat kernels. Roasting was correlated with a decrease in wheat density. FBR demonstrated to be a superior roasting method in terms of product quality, since these samples indicated a better heat transfer and more uniform texture than sand roasted kernels. A previous study on grain roasting (both sand and microwave) indicated that decreased bulk densities were due to a loss in structural integrity between starch-protein and starch-starch matrices and this was attributed to the formation of air spaces in the endosperm (Sharma and Gujral, 2011). The higher puffing effect that occurred during oven roasting resulted in larger air volumes (porosity) and lower relative densities in comparison to FCCT roasting. Decreased densities was an indication of pore formation due to volumetric expansion (Kahyaoglu et al., 2010). This study confirmed the negative relationship between porosity and density.

4. Conclusion

It was possible to successfully illustrate distinct changes and differences in the microstructure of wheat kernels induced by the two roasting methods from the 2D projection images, which could be rendered into 3D volumes to perform quantitative analysis. The degree of cracking and cavities in the wheat kernels provided an indication of the complexity and interconnectedness of the porous network. Cavities were much larger in the oven-roasted samples resulting in more open porous and expanded structure in relation to FCCT roasting, which had a less destructive impact. The qualitative results observed in the 2D images were confirmed with quantitative measurements. Roasting resulted in an increase in volume, porosity and ER and a decrease in relative density. These measurements were higher during oven roasting. Oven roasting, in a static position, resulted in unevenly roasted kernels, thus the advantage of FCCT roasting is that the product is continuously rotating in the superheated steam and the kernel surface is exposed uniformly. Therefore FCCT roasting is preferable in terms of minimal structural alteration caused during roasting, resulting in a more acceptable internal structure. The material density also remained constant during FCCT roasting which will lead to less affected milling yields.

X-ray μCT is increasingly being used as a research tool to study the microstructure of agricultural produce since it enables non-destructive capturing of high-resolution images, permitting fine details to be studied. This technique has been demonstrated to be a powerful tool to investigate and characterise the microstructure of roasted wheat.

Acknowledgments

Financial assistance was provided by the National Research Foundation (NRF) (Grant specific unique reference number (UID) 76641 and 88057) and the Winter Cereal Trust (study grant for Letitia Schoeman). The authors acknowledge the KU Leuven and Stellenbosch University Staff Exchange Programme for enabling a research visit of Marena Manley to the research group of Prof Bart Nicolaï (BIOSYST-MeBioS, KU Leuven, Willem de Croylaan 42, 3001 Leuven, Belgium) as well as Prof Nicolaï and Dr Pieter Verboven for hosting M Manley and valuable contributions.

References

Agbisit, R., Alavi, S., Cheng, E., Herald, T., Trater, A., 2007. Relationships between microstructure and mechanical properties of cellular cornstarch extrudates. J. Texture Stud. 38 (2), 199–219.

Aguilera, J.M., 2005. Why food microstructure? J. Food Eng. 67 (1), 3–11.

Al-Mahasneh, M.A., Rababah, T.M., 2007. Effect of moisture content on some physical properties of green wheat. J. Food Eng. 79 (4), 1467–1473.

Almeida-Dominguez, H.D., Suhendro, E.L., Rooney, L.W., 1997. Factors affecting rapid visco analyser curves for the determination of maize kernel hardness. J. Cereal Sci. 25 (1), 93–102.

Andrejko, D., Grochowicz, J., Goździewska, M., Kobus, Z., 2011. Influence of infrared treatment on mechanical strength and structure of wheat grains. Food Bioprocess Technol. 4 (8), 1367–1375.

Baiano, A., Fares, C., Peri, G., Romaniello, R., Taurino, A.M., Siciliano, P., Gambacorta, G., Lamacchia, C., Pati, S., Notte, E.L., 2008. Use of a toasted durum whole meal in the production of a traditional Italian pasta: chemical, mechanical, sensory and image analyses. Int. J. Food Sci. Technol. 43 (9), 1610–1618.

Bayram, M., Öner, M.D., Eren, S., 2004. Effect of cooking time and temperature on the dimensions and crease of the wheat kernel during bulgur production. J. Food Eng. 64 (1), 43–51.

Bellido, G.G., Scanlon, M.G., Page, J.H., Hallgrimsson, B., 2006. The bubble size distribution in wheat flour dough. Food Res. Int. 39 (10), 1058–1066.

Besbes, E., Jury, V., Monteau, J.Y., Le Bail, A., 2013. Characterizing the cellular structure of bread crumb and crust as affected by heating rate using X-ray microtomography. J. Food Eng. 115 (3), 415–423.

Chang, C., 1988. Measuring density and porosity of grain kernels using a gas pycnometer. Cereal Chem. 65 (1), 13–15.

Chevallier, S., Réguerre, A.L., Le Bail, A., Della Valle, G., 2014. Determining the cellular structure of two cereal food foams by X-ray micro-tomography. Food Biophys. 9, 219–228.

Demirkesen, I., Kelkar, S., Campanella, O.H., Sumnu, G., Sahin, S., Okos, M., 2014. Characterization of structure of gluten-free breads by using X-ray microtomography. Food Hydrocoll. 36, 37–44.

Dobraszczyk, B., Whitworth, M., Vincent, J., Khan, A., 2002. Single kernel wheat hardness and fracture properties in relation to density and the modelling of fracture in wheat endosperm. J. Cereal Sci. 35 (3), 245–263.

Dogan, H., 2007. Nondestructive imaging of agricultural products using X-ray microtomography. Microsc. Microanal. 13, 1316–1317.

Donis-González, I.R., Guyer, D.E., Fulbright, D.W., Pease, A., 2014. Postharvest noninvasive assessment of fresh chestnut (*Castanea* spp.) internal decay using computer tomography images. Postharvest Biol. Technol. 94 (0), 14–25.

Donis-González, I.R., Guyer, D.E., Chen, R., Pease, A., 2015. Evaluation of undesirable fibrous tissue in processing carrots using Computed Tomography (CT) and structural fiber biochemistry. J. Food Eng. 153, 108–116.

Du Plessis, A., Seifert, T., Booysen, G., Els, J., 2014. Microfocus X-ray computed tomography (CT) analysis of laser sintered parts. South Afr. J. Ind. Eng. 25, 39–49.

Dutra, E., Oliveira, L., Franca, A., Ferraz, V., Afonso, R., 2001. A preliminary study on the feasibility of using the composition of coffee roasting exhaust gas for the determination of the degree of roast. J. Food Eng. 47 (3), 241–246.

Evers, T., Millar, S., 2002. Cereal grain structure and development: some implications for quality. J. Cereal Sci. 36 (3), 261–284.

Fang, C., Campbell, G.M., 2000. Effect of measurement method and moisture content on wheat kernel density measurement. Food Bioprod. Process. 78 (4), 179–186.

FAOSTAT, 2015. Food and Agriculture Organization of the United Nations. Statistics division [Internet document]. URL. http://faostat3.fao.org/download/Q/QC/E (accessed 07.05.15.).

Flinn, B., 2012. New Roasting Technology! [Internet document]. URL. http://www.agriculture.com/machinery/precision-agriculture/new-roasting-technology_234-ar26331?print (accessed 24.02.14.).

Frisullo, P., Barnabà, M., Navarini, L., Del Nobile, M., 2012. *Coffea arabica* beans microstructural changes induced by roasting: an X-ray microtomographic investigation. J. Food Eng. 108 (1), 232–237.

Hernández, J.A., Heyd, B., Trystram, G., 2008. Prediction of brightness and surface area kinetics during coffee roasting. J. Food Eng. 89 (2), 156–163.

Horvat, M., Guthausen, G., Tepper, P., Falco, L., Schuchmann, H.P., 2014. Non-destructive, quantitative characterization of extruded starch-based products by magnetic resonance imaging and X-ray microtomography. J. Food Eng. 124, 122–127.

Işikli, N.D., Şenol, B., Çoksöyler, N., 2014. Some physical and mechanical properties of roasted zerun wheat. J. Food Sci. Technol. 51, 1990–1997.

Jha, S., 2005. Mathematical simulation of roasting of grain. J. Food Eng. 71 (3), 304–310.

Jones, D., Chinnaswamy, R., Tan, Y., Hanna, M., 2000. Physiochemical properties of ready-to-eat breakfast cereals. Cereal Foods World 45 (4), 164–168.

Kahyaoglu, L.N., Sahin, S., Sumnu, G., 2010. Physical properties of parboiled wheat and bulgur produced using spouted bed and microwave assisted spouted bed drying. J. Food Eng. 98 (2), 159–169.

Kayitesi, E., Duodu, K.G., Minnaar, A., de Kock, H.L., 2010. Sensory quality of marama/sorghum composite porridges. J. Sci. Food Agric. 90 (12), 2124–2132.

Kelkar, S., Boushey, C.J., Okos, M., 2015. A method to determine the density of foods using X-ray imaging. J. Food Eng. 159, 36–41.

Ketcham, R.A., Carlson, W.D., 2001. Acquisition, optimization and interpretation of X-ray computed tomographic imagery: applications to the geosciences. Comput. Geosci. 27 (4), 381–400.

Kheiralipour, K., Karimi, M., Tabatabaeefar, A., Naderi, M., Khoubakht, G., Heidarbeigi, K., 2008. Moisture-depend physical properties of wheat (*Triticum aestivum* L.). J. Agric. Technol. 53, 53–64.

Köksel, H., Sivri, D., Scanlon, M., Bushuk, W., 1998. Comparison of physical properties of raw and roasted chickpeas (leblebi). Food Res. Int. 31 (9), 659–665.

Lamacchia, C., Baiano, A., Lamparelli, S., Notte, E.L., Luccia, A.D., 2010. Changes in durum wheat kernel and pasta proteins induced by toasting and drying processes. Food Chem. 118 (2), 191–198.

Lammertyn, J., Dresselaers, T., Van Hecke, P., Jancsók, P., Wevers, M., Nicolai, B., 2003. MRI and X-ray CT study of spatial distribution of core breakdown in 'Conference' pears. Magn. Reson. Imaging 21 (7), 805–815.

Landis, E.N., Keane, D.T., 2010. X-ray microtomography. Mater. Charact. 61 (12), 1305–1316.

Landis, E.N., Nagy, E.N., Keane, D.T., 2003. Microstructure and fracture in three dimensions. Eng. Fract. Mech. 70 (7), 911–925.

Lazar, M., Mossman, A., Wallace, J., 1974. Air-fluidized toasting of whole kernel wheat-processing variables and functional properties for food applications. J. Food Sci. 39 (2), 239–243.

Lee, E.Y., Lim, K.I., Lim, J., Lim, S.T., 2000. Effects of gelatinization and moisture content of extruded starch pellets on morphology and physical properties of microwave-expanded products. Cereal Chem. 77 (6), 769–773.

Léonard, A., Blacher, S., Nimmol, C., Devahastin, S., 2008. Effect of far-infrared radiation assisted drying on microstructure of banana slices: an illustrative use of X-ray microtomography in microstructural evaluation of a food product. J. Food Eng. 85 (1), 154–162.

Licciardello, F., Frisullo, P., Laverse, J., Muratore, G., Del Nobile, M.A., 2012. Effect of sugar, citric acid and egg white type on the microstructural and mechanical properties of meringues. J. Food Eng. 108 (3), 453–462.

Mariotti, M., Alamprese, C., Pagani, M.A., Lucisano, M., 2006. Effect of puffing on ultrastructure and physical characteristics of cereal grains and flours. J. Cereal Sci. 43 (1), 47–56.

Mendoza, F., Verboven, P., Mebatsion, H.K., Kerckhofs, G., Wevers, M., Nicolaï, B., 2007. Three-dimensional pore space quantification of apple tissue using X-ray computed microtomography. Planta 226 (3), 559–570.

Mohorič, A., Vergeldt, F., Gerkema, E., Dalen, G.v., Doel, L.R.v.d., Vliet, L.J.v., As, H.V.,

Duynhoven, J.v, 2009. The effect of rice kernel microstructure on cooking behaviour: a combined μ-CT and MRI study. Food Chem. 115 (4), 1491–1499.
Moreira, R.G., 2001. Impingement drying of foods using hot air and superheated steam. J. Food Eng. 49 (4), 291–295.
Mossman, A., Rockwell, W., Fellers, D., 1973. Hot air toasting and rolling whole wheat effect on organoleptic, physical and nutritional quality. J. Food Sci. 38 (5), 879–884.
Murthy, K.V., Ravi, R., Keshava Bhat, K., Raghavarao, K.S.M.S., 2008. Studies on roasting of wheat using fluidized bed roaster. J. Food Eng. 89 (3), 336–342.
Ndungu, K.E., Emmambux, M.N., Minnaar, A., 2012. Micronisation and hot air roasting of cowpeas as pretreatments to control the development of hard-to-cook phenomenon. J. Sci. Food Agric. 92 (6), 1194–1200.
Neethirajan, S., Karunakaran, C., Jayas, D., White, N., 2006. X-ray computed tomography image analysis to explain the airflow resistance differences in grain bulks. Biosyst. Eng. 94 (4), 545–555.
Nelson, S., 2015. Dielectric Properties of Agricultural Materials and Their Applications. Academic Press, London, pp. 260–261.
Nyembwe, P., Minnaar, A., Duodu, K.G., de Kock, H.L., 2015. Sensory and physicochemical analyses of roasted marama beans [*Tylosema esculentum* (Burchell) A. Schreiber] with specific focus on compounds that may contribute to bitterness. Food Chem. 178, 45–51.
Ohm, J., Chung, O., Deyoe, C., 1998. Single-kernel characteristics of hard winter wheats in relation to milling and baking quality 1. Cereal Chem. 75 (1), 156–161.
Pardeshi, I., Chattopadhyay, P., 2010. Hot air puffing kinetics for soy-fortified wheat-based ready-to-eat (RTE) snacks. Food Bioprocess Technol. 3 (3), 415–426.
Pittia, P., Sacchetti, G., Mancini, L., Voltolini, M., Sodini, N., Tromba, G., Zanini, F., 2011. Evaluation of microstructural properties of coffee beans by synchrotron X-ray microtomography: a methodological approach. J. Food Sci. 76 (2), 222–231.
Salvo, L., Suéry, M., Marmottant, A., Limodin, N., Bernard, D., 2010. 3D imaging in material science: application of X-ray tomography. Comptes Rendus Phys. 11, 641–649.
Sharma, P., Gujral, H.S., 2011. Effect of sand roasting and microwave cooking on antioxidant activity of barley. Food Res. Int. 44 (1), 235–240.
Sumithra, B., Bhattacharya, S., 2008. Toasting of corn flakes: product characteristics as a function of processing conditions. J. Food Eng. 88 (3), 419–428.
Suresh, A., Neethirajan, S., 2015. Real-time 3D visualization and quantitative analysis of internal structure of wheat kernels. J. Cereal Sci. 63, 81–87.
Umbaugh, S.E., 2011. Digital image processing and analysis: human and computer vision applications with CVIPtools. CRC Press, Boca Raton, pp. 456–463.
Vadivambal, R., Jayas, D.S., 2007. Changes in quality of microwave-treated agricultural products—a review. Biosyst. Eng. 98 (1), 1–16.
Van Dalen, G., Nootenboom, P., Van Vliet, L.J., 2007. 3D Imaging, analysis and modelling of porous cereal products using X-ray microtomography. Image Anal. Stereol. 26, 169–177.
Van Dyck, T., Verboven, P., Herremans, E., Defraeye, T., Van Campenhout, L., Wevers, M., Claes, J., Nicolaï, B., 2014. Characterisation of structural patterns in bread as evaluated by X-ray computer tomography. J. Food Eng. 123, 67–77.
Verboven, P., Kerckhofs, G., Mebatsion, H.K., Ho, Q.T., Temst, K., Wevers, M., Cloetens, P., Nicolaï, B.M., 2008. Three-dimensional gas exchange pathways in pome fruit characterized by synchrotron X-ray computed tomography. Plant Physiol. 147 (2), 518–527.
Wang, S., Austin, P., Bell, S., 2011. It's a maze: the pore structure of bread crumbs. J. Cereal Sci. 54 (2), 203–210.
Witek, M., Węglarz, W.P., de Jong, L., van Dalen, G., Blonk, J.C.G., Heussen, P., Van Velzen, E., Van As, H., van Duynhoven, J., 2010. The structural and hydration properties of heat-treated rice studied at multiple length scales. Food Chem. 120 (4), 1031–1040.
Zhu, L.J., Dogan, H., Gajula, H., Gu, M.H., Liu, Q.Q., Shi, Y.C., 2012. Study of kernel structure of high-amylose and wild-type rice by X-ray microtomography and SEM. J. Cereal Sci. 55 (1), 1–5.